Korean J. Chem. Eng., **27**(2), 697-704 (2010)
DOI: 10.1007/s11814-010-0106-x

Fabrication of CdS thin films assisted by Langmuir deposition, self-assembly, and dip-pen nanolithography

Gil Sun Lee*,, Ji Hwon Lee*, Hyun Choi*, and Dong June Ahn*,†**

*Department of Chemical and Biological Engineering, Korea University, Seoul 136-701, Korea
**Center for Integrated-Nano-Systems, Korea University, Seoul 136-701, Korea
(*Received 14 October 2009 • accepted 23 November 2009*)

Abstract−Thin CdS films were fabricated by Langmuir deposition, self-assembly, and dip-pen nanolithography methods. Firstly, LB films of saturated arachidic acid and LS films of unsaturated 10,12-pentacosadiynoic acid were reacted with cadmium ions and exposed to H_2S gas. Formation of CdS crystal was observed with Fourier transform infrared (FTIR) spectra and atomic force microscope (AFM). Secondly, mercaptohexadecanoic acid was self-assembled on Au substrate and was reacted with CdS colloidal particles. At pH=9.1, the density of CdS colloids immobilized on Au substrate was very high compared to one at pH=5.0. Finally, thin films of CdS were also prepared on silicon and Au substrates by cadmium chloride-coated AFM tip and successive exposure of H_2S gas. Localized formation of CdS crystal was suggested with AFM and depth-profiling Auger electron microscopy (AES).

Key words: CdS, Langmuir-Blodgett Film, Langmuir-Schafer Film, Self-assembled Monolayers, Dip-pen Nanolithography

INTRODUCTION

Renewable energy generated from natural resources such as sunlight, wind, tides, geothermal heat, etc. has been much investigated for it can reserve Earth from global warming by reducing environmental pollutants. Especially, solar cells have attracted a great deal of interest in both academic researches and industrial needs. Many materials including silicon, II-IV semiconductor compounds, carbon nanotube, graphene, etc. have been used to make heterojunction-based solar cells. Among these materials, cadmium sulfide (CdS) is a representative due to its wideband gap of 2.42 eV at room temperature, good photoconduction, high electron affinity, and inexpensive preparation [1-4]. Methods for generating CdS include chemical vapor deposition, laser deposition, electrochemical deposition, and precipitation [5-7].

For the past decades, many organic materials have been reported to be coated on substrates with nanometer-scale by Langmuir-Blodgett (LB) [8,9], Langmuir-Schafer (LS) [10,11], and self-assembled monolayers (SAMs) [12,13]. Such organic templates prepared by these methods can offer better control of the molecular density of surface functional on which CdS nanoparticles are deposited and have an advantage of lower preparation costs due to their mild process conditions at normal temperature and pressure.

On the other hand, direct coating methods such as microcontact printing (μCP) [14,15], nanoimprinting [16,17], scanning probe lithography (SPL) [18,19] e-beam lithography [20] have been investigated to accurately deposit organic materials in nanometer-scales for applications to nanometer-scale molecular electronics and devices possessing advanced functions. In addition to the miniaturization, the fabrication of nanometer-scale domain on a target position over surfaces is beginning to play an important role in related fields. Recently, dip-pen nanolithography (DPN) [21-24] technique invented by Mirkin et al. has been widely used in various fields due to its ability to deposit accurate nano-pattern of both organic and inorganic materials.

In this work, we report a variety of routes to simple deposition of CdS thin films by Langmuir deposition, self-assembly, and DPN methods at room temperature. Firstly, LB films of saturated arachidic acid and LS films of unsaturated 10,12-pentacosadiynoic acid were reacted with cadmium ions and exposed to H_2S gas for 1 h. Formation of CdS thin films was confirmed with FTIR spectra and AFM. Secondly, mercaptohexadecanoic acid was self-assembled on Au substrate and was reacted with CdS colloidal particles. At pH=9.1, the density of immobilized CdS colloids was very much higher than one at pH=5.0. Finally, thin nanometer-scale CdS crystals with predetermined pattern at target local positions were prepared on silicon and Au substrates using dip-coated AFM tips. Localized formation of CdS crystal lines with width less than 50 nm was confirmed with AFM and AES after exposure of H_2S gas for 1 h. These methods to form thin CdS films could be potentially applicable to increase photo-responsive electronic devices.

EXPERIMENTAL SECTION

1. Materials

Arachidic acid (eicosanoic acid; 99%) and 10,12-pentacosadiynoic acid (PCDA; 99%) were purchased from Aldrich and Farchan Laboratory, respectively. Chloroform (99.8%), ethanol (99.8%), and 16-mercaptohexadecanoic acid (MHA; 90%) were purchased from Fluka. Cadmium chloride ($CdCl_2$; 99.9%) and sodium mercaptoacetate (99%) were obtained from Aldrich and Sigma, respectively. All surfactants and solvents were used without further purification.

†To whom correspondence should be addressed.
E-mail: ahn@korea.ac.kr
‡This paper is dedicated to Professor Jae Chun Hyun for celebrating his retirement from Department of Chemical and Biological Engineering of Korea University.

Deionized (DI) water with a resistivity of 18.2 MΩ·m was used as a solvent. Silicon dioxide (SiO_2) was used as substrates for DPN.

2. Surface Isotherm

An aliquot of chloroform solution containing 1 mM arachidic acid and 10,12-pentacosadiynoic acid was spread onto the air/water interface of a KSV Langmuir trough (KSV minitrough, Finland) containing deionized water as a subphase. After chloroform was evaporated for 20 min, the molecules were compressed to obtain surface isotherms at the barrier speed of 10 mm/min. To obtain the isotherm of cadmium adsorption, DI water solution containing 1 mM $CdCl_2$ was used as the subphase of a KSV Langmuir trough.

3. Fabrication of Langmuir-Blodgett (LB)/Langmuir-Schaefer (LS) Films

Arachidic acid (1 mM) molecules after evaporating chloroform were compressed to form the close-packed monolayer at the surface pressure of 20 mN/m. After waiting for 20 min to reach the equilibrium, the monolayer was deposited onto a hydrophobic octadecytriethoxysilane (OTE) and a clean calcium fluoride (CaF_2) substrate at the dipper speed of 10 mm/min. The thickness of these LB film was controlled by dipping times. Meantime, PCDA molecules were deposited onto an OTE substrate by Langmuir-Schaefer method due to a collapse induced during the compression to obtain the isotherm.

4. Fabrication of CdS Colloid Particles

CdS colloid particles are fabricated as follows. First, 500 ml of 1 mM $CdCl_2$ and 500 ml of 1.6 mM $C_2H_3O_2SNa$ (sodium mercaptoacetate) were mixed and the solution was turbid blue. Second, the pH of the solution was adjusted below pH=3.35 by adding 1 N HCl aqueous solution and the solution was colorless. Third, rapid stirring after addition of 150 ml of 10 mM Na_2S (Sodium sulfide) to the sample solution made the solution yellow. Finally, water-soluble yellow CdS colloid particles were obtained by using a rotary evaporator.

5. Fabrication of Self-assembled Monolayers (SAMs)

MHA molecules are chosen as a template of organic fatty acid due to higher surface density compared to the LB and LS films. Thiol group (SH) of MHA molecule is self-assembled on the gold substrate by a covalent bond. MHA SAMs are fabricated by dipping a clean gold substrate on 2 mM MHA/ethanol solution for 4 h.

6. AFM Tip Coating with Inorganic Materials

A silicon nitride tip (Si_3N_4; ThermoMicroscopes, sharpened Microlever A, force constant=0.05 N/m) was used to DPN experiment. To increase the hydrophilicity of the tip, wet oxidation was performed as followed. First, the tip was treated by sonication for 20 min in $NH_4OH : H_2O_2 : H_2O$ (1 : 1 : 5 by volume). Next, it was sonicated in DI water for 5 min and blown dry with N_2 gas. Conventional tips and hydrophilic tips were dipped in 10 mM and saturated $CdCl_2$ solution for 10 min. The tip was blown dry by using a light stream of nitrogen gas (99.99%).

7. Fabrication Methods of CdS Semiconductor Thin Films

To fabricate semiconductor CdS thin films, three methods were used: an organic template-induced method, a method using CdS colloid particles, and DPN method using inorganic $CdCl_2$-coated AFM tips.

8. Instruments (FTIR, SEM, AFM and AES)

Transmission FTIR (Perkin-Elmer, Spectrum GX1) was used to confirm whether CdS thin films were formed on the substrates. Inorganic coated AFM tips were investigated with FE-SEM (Field emission-scanning electron microscope; Hitachi, S-4300). All DPN experiments were carried out with a CP AFM (ThermoMicroscopes; USA) with a combined AFM/LFM head at ambient temperature and conventional Si_3N_4 tips. To minimize piezo tube drift problems, a 100-μm scanner with closed loop scan control was used for all experiments. Auger electron spectra and AES depth profiles were obtained with a model - Physical Electronics (PHI 680 Auger Nanoprobe; USA). The residual gas pressure in the chamber during imaging was 1×10^{-10} Torr.

RESULTS AND DISCUSSION

1. Formation of CdS Thin Films by Precursor Reactions with LB and LS Organic Templates

As an organic template for inducing CdS thin films, Langmuir monolayers of saturated arachidic acid and unsaturated PCDA were used. It is well known that arachidic acid easily forms Langmuir monolayer at air/water interface and PCDA are polymerized upon exposure of UV light (254 nm). Fig. 1 shows the surface isotherms of arachidic acid at air/water interface on pure water (pH=5.5) and on cadmium ionic aqueous solution (1 mM, pH=5.5).

According to decrease of mean molecular area (MMA), the surface isotherm of Fig. 1(a) provides the arachidic acid molecules are in liquid-expanded (ca. 30 $Å^2$/molecule), liquid-condensed (30-19 $Å^2$/molecule), and solid-like state (below 19 $Å^2$/molecule). In the solid-like state, the arachidic acid monolayer is known to organize in a close-packed fashion [25]. On the other hand, the adsorption of cadmium ions to the carboxylic acid of the arachidic acid monolayer removes liquid-condensed state and steeply changes from liquid-expanded state to solid-like state as shown in Fig. 1(b). More adsorption of cadmium ions to the arachidic acid monolayers is beneficial for growth of the CdS crystals on the organic template. Therefore, a concentration of 1 mM was used, because above 80% adsorption of cadmium ions was reported in 1 mM by Hyun et al. [26].

CdS crystals are grown after exposure H_2S gas to LB films of arachidate monolayer, i.e., arachidic acid monolayer adsorbed cadmium ions. Fig. 2 shows FTIR spectra of CdS growth in the arachidic acid template. First, spectrum I was obtained from LB films of arachidic acid, which contains carbonyl stretching band (νC=O) at

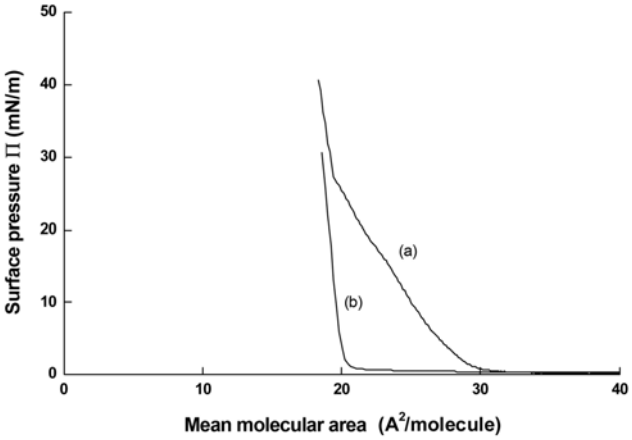

Fig. 1. Surface isotherms of arachidic acid monolayers on pure water (a) and on cadmium (1 mM) ionic aqueous solution (b).

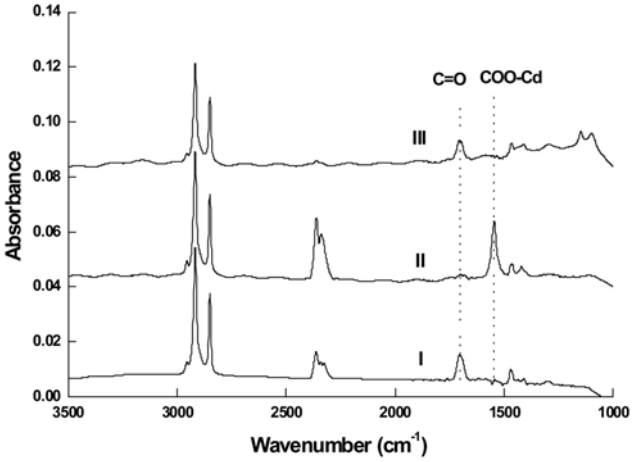

Fig. 2. FTIR transmission spectra. (I) Arachidic acid LB film, (II) Cadmium arachidate LB film, and (III) After exposure of the film (II) to H_2S gas for 1 h.

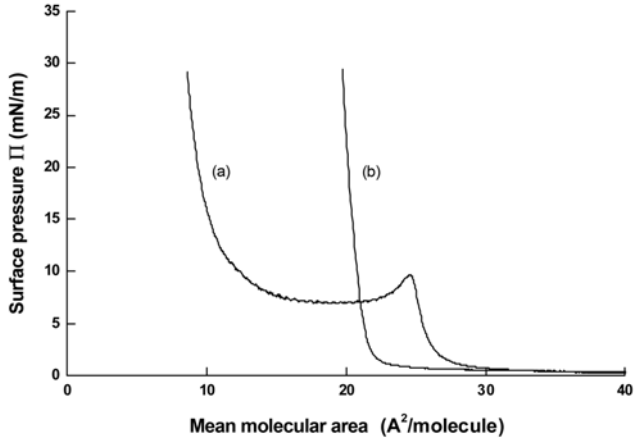

Fig. 4. Surface isotherms of PCDA monolayers on pure water (a) and on Cd (1 mM) ionic aqueous solution (b).

1,703 cm^{-1}. In case of arachidic acid monolayers, multilayer deposition by LB technique is imperfect. Therefore, cadmium arachidate monolayers which cadmium ion adsorbed on arachidic acid monolayers were used to deposit multilayer LB films. Spectrum II of 10-layer LB films deposited on hydrophobic CaF_2 substrate shows existence of asymmetric carboxylate band (νCOO-Cd) at 1,546 cm^{-1} and complete disappearance of carbonyl stretching band, indicating pure cadmium arachidate LB film are transferred on the substrates [26]. After exposure of the LB films to H_2S gas, the carbonyl stretching band increases and the asymmetric carboxylate band decreases as shown in spectrum III. These spectra demonstrate the template is reduced from cadmium arachidate to arachidic acid by reaction between cadmium ions and sulfides. The mechanism of the reaction is as follows [27].

$$(C_{19}COO^-)_2\text{-}Cd^{2+}+H_2S \rightarrow 2C_{19}COOH+CdS$$

To investigate the change of the surface roughness as CdS thin films were grown, 9-layer LB films deposited on hydrophilic mica substrate were analyzed with AFM. Fig. 3 shows that the surface roughness increases from 2.6 Å to 7.3 Å after CdS growth, indicating crystal growth induces a surface rougher than cadmium arachidate LB films.

Fig. 4 presents the surface isotherm of PCDA monolayers on pure water and on cadmium (1 mM) ionic aqueous solution. Fig. 4(a) shows PCDA Langmuir monolayer collapses at an MMA of ca. 24 $Å^2$/molecule. Further compression of surface area leads to a stable multilayered films and the PCDA molecule at ca. 8 $Å^2$ is average 3-layers. On the contrary, Fig. 4(b) shows an adsorption of Cd ion to the carboxylic acid of PCDA molecule increases the stability of PCDA monolayer, and the isotherm is similar to one of cadmium arachidate monolayers as shown in Fig. 2(b). In case of pure PCDA, the PCDA monolayer was over-compressed to form multilayered (surface pressure=30 mN/m) and polymerized by irradiation with the 254 nm-UV light (1 mW/cm^2) for 30 s to give blue-colored films. The films were transferred to hydrophobized glass slides precoated with octadecyltriethoxysilane (OTE) through the horizontal-touch

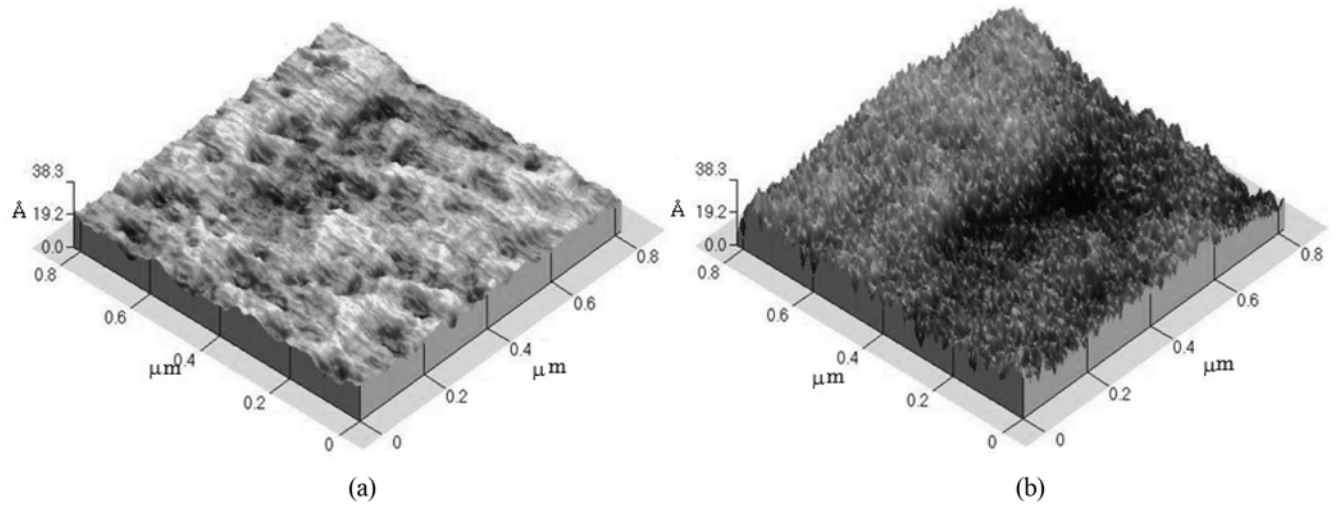

Fig. 3. AFM images for a 9-layer cadmium arachidate LB film on mica (a) and a CdS film grown on the LB film (b). Rms roughness= 2.58 Å (a) and 7.34 Å (b).

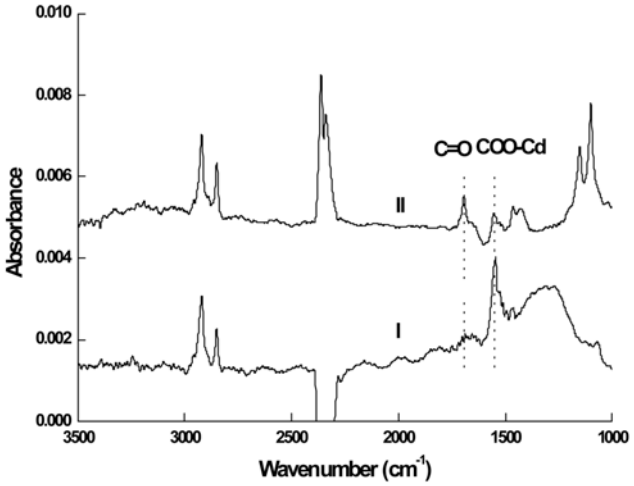

Fig. 5. FTIR spectra of CdS growth on PCDA-Cd (1 mM) LS monolayer deposited at surface pressure=30 mN/m. (I) PCDA-Cd (1 mM) Langmuir-Schaefer monolayer and (II) after exposure of the monolayer to H_2S gas for 1 h.

Langmuir-Schaefer method. Fig. 5 shows FTIR spectra of CdS growth on PCDA-Cd (1 mM) LS monolayer deposited at surface pressure= 30 mN/m. Spectrum I has only existence of the asymmetric carboxylate stretching band in head-group region, indicating all carboxylic acid groups react with Cd ions. After exposure of the LS films to H_2S gas, spectrum II shows the carbonyl stretching band increases and the asymmetric carboxylate stretching band decreases at the same time. These results are in good agreement with ones in arachidic acid of Fig. 2 and suggest PCDA-Cd LS monolayer could be used as an organic template for CdS growth.

2. Fabrication of CdS Thin Films by Deposition of Colloid Particles

Fig. 6 shows AFM images of CdS colloidal particles fabricated by solution casting. Immobilized CdS colloidal particles are irregular and the density of the particles is not uniform as shown in Fig. 6(a). In the magnification image, the size of CdS colloidal particles ranged from 60 nm to 100 nm (Fig. 6(b)). These AFM images suggest that solution casting is not a reliable method for deposition of CdS particles. To overcome such demerit, the deposition of CdS particles by LB technique is tried at air/water interface because it is

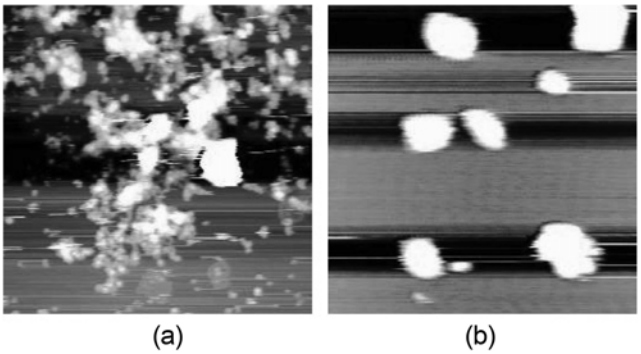

Fig. 6. AFM images of CdS colloidal particles immobilized by solution casting ((a) 3×3 μm^2 and (B) 0.5×0.5 μm^2) on mica surfaces.

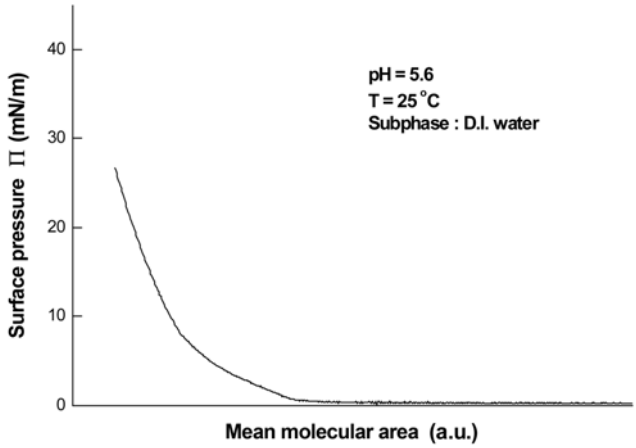

Fig. 7. Surface iostherm of CdS colloidal particles.

reported that a deposition of water-soluble proteins by LB method is possible at air/water interface [28]. The surface isotherm of CdS colloidal particles shows the surface density of CdS particles is very high from the fact that the surface pressure is above 20 mN/m (Fig. 7).

Fig. 8 shows the AFM and lateral force microscope (LFM) images of CdS colloidal particles by LB deposition formed on mica surfaces. The images present two characteristic areas of CdS colloidal particles, that is, one is well deposited, the other is not coated. LFM image of Fig. 8(b) suggests the CdS regular particles are arrayed although particle arrays are not shown in topography of Fig. 8(a). These results suggest the deposition of CdS particles by LB technique is successful to form arrayed CdS particles although uniformity of the thin films is not satisfactory.

To increase the density of the surface, MHA molecules as an organic template are chosen to immobilize CdS colloidal particles. MHA SAMs are fabricated by dipping a clean gold substrate on 2 mM MHA/ethanol solution for 4 h. Then, CdS colloidal particles are immobilized on the carboxyl acid group (-COOH) of SAMs at pH=5.0 and 9.1. Fig. 9(a) and (b) show a representative topography and LFM image of CdS colloidal particles immobilized on Au/MHA surfaces at pH=5.5 of colloidal solution. LFM image shows that a clear shape of CdS particles is well distributed on the substrate compared to CdS LB films in Fig. 8(a). To investigate the effect of deprotonation on immobilization of CdS particles, the immobilization was performed at pH=9.1. Fig. 9(c, d) shows the density of CdS par-

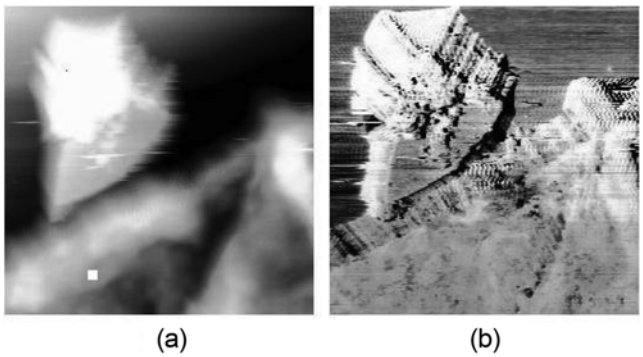

Fig. 8. AFM (a) and LFM (b) images of CdS colloidal particles by LB deposition (10×10 μm^2) formed on mica surfaces.

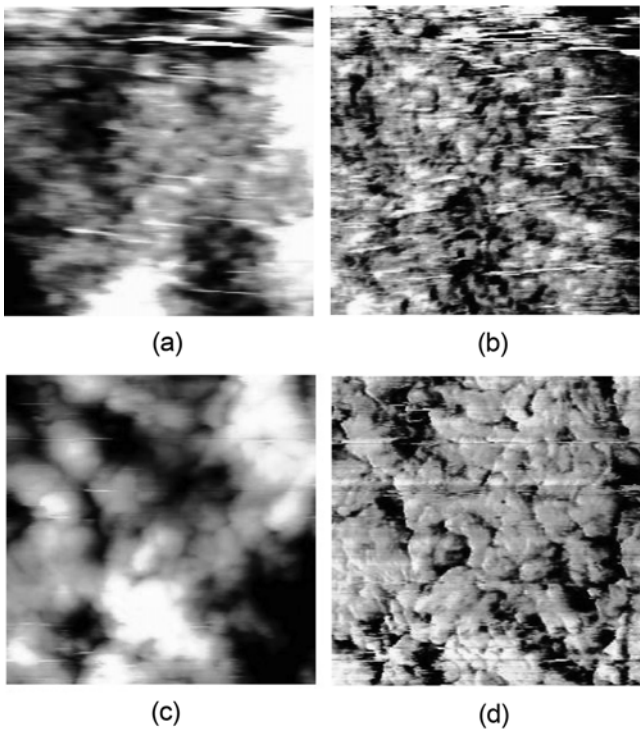

Fig. 9. CdS colloidal particles immobilized on Au/MHA surfaces: (a) topographic image and (b) lateral force image (1×1 μm^2) at pH=5.5 of colloidal solution, (c) topographic image, and (d) lateral force image (1×1 μm^2) at pH=9.1.

ticles is relatively increased as compared to one at pH=5.0 (Fig. 9(a, b)), indicating the pH of CdS colloidal solution plays an important role in increasing the density of CdS particles.

3. Patterning of CdS Thin Film by Dip-pen Nanolithography (DPN)

SEM images of bare AFM tip (a) and $CdCl_2$-coated AFM tip (b) confirm $CdCl_2$ are well coated on the surface of AFM tip as shown in Fig. 10. Fig. 11 shows LFM images of CdS square (a) and lines (b) formed via dip pen nanolithography (DPN) and AES spectra of silicon dioxide (c) and CdS surfaces (d). The square and lines are formed as follows. First, the square and lines of cadmium chloride are deposited on a silicon dioxide (SiO_2) substrate by scanning the cadmium chloride coated tip over the 20×20 μm^2 area at a scan rate of 1 Hz for 2 h and by vertically scanning the tip for 1, 5, and 30 min (left to right) at a scan rate of 1 Hz, respectively. Then CdS patterns are formed after exposure to H_2S for 1 h. Fig. 11(a) shows an LFM image of the square within a larger scan area (25 μm by 25 μm) displays two areas of different contrast. The interior dark area is CdS, and the exterior light area is SiO_2. Fig. 11(b) shows the line width of CdS are 50, 80, and 100 nm from left to right, respectively. The above LFM images, however, do not show whether CdS crystals are really formed on the desired substrates because there is no proof by X-ray diffractometer (XRD), STM, etc. Since the CdS area is so small and its thickness is very thin, it is difficult to analyze from XRD measurement whether CdS crystal is produced. Therefore, we investigated the existence of CdS using an AES. Fig. 11(c) and (d) show AES multiple spectra of cadmium and sulfur atom in SiO_2 surface and CdS formed by DPN on silicon dioxide. From the spectra, it might be suggested that H_2S gas reacts with $CdCl_2$ and then creates CdS crystals.

To have a better confirmation, the depth-profiling of CdS deposited in bulk state was analyzed. First, $CdCl_2$ is deposited on a gold substrate by solution casting. Then, H_2S gas is exposed on the samples for 2 h. Fig. 12 shows the AFM images before and after H_2S gas reaction and AES results in two positions on the gold substrate. Thin layer shown in Fig. 12(b) is presumed CdS crystals formed after reaction. Also, AES spectra (c) appear that sulfur atom in point 1 (a local position of thinner layer) is relatively more than one in point 2 (a local position of thicker layer). It means that the reaction from $CdCl_2$ to CdS in the edge is more active. Meanwhile, the AES depth profiles of two positions are shown in Fig. 13. The depth profile in precipitate of $CdCl_2$ shows that chloride concentration in surface of precipitate is higher than one in the inner of precipitate (Fig. 13(a)).

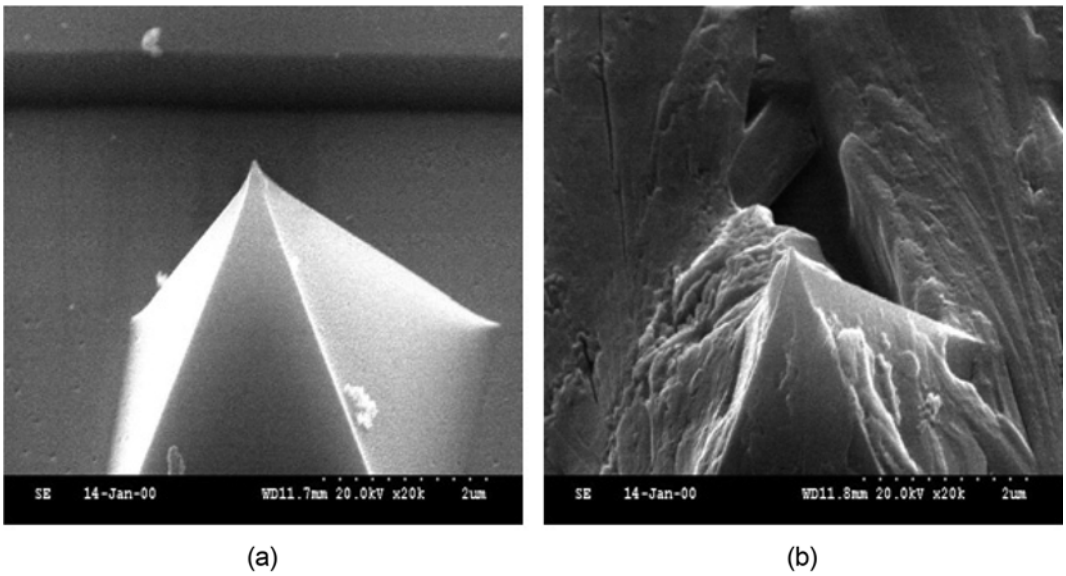

Fig. 10. SEM images of bare AFM tip (a) and $CdCl_2$-coated AFM tip (b).

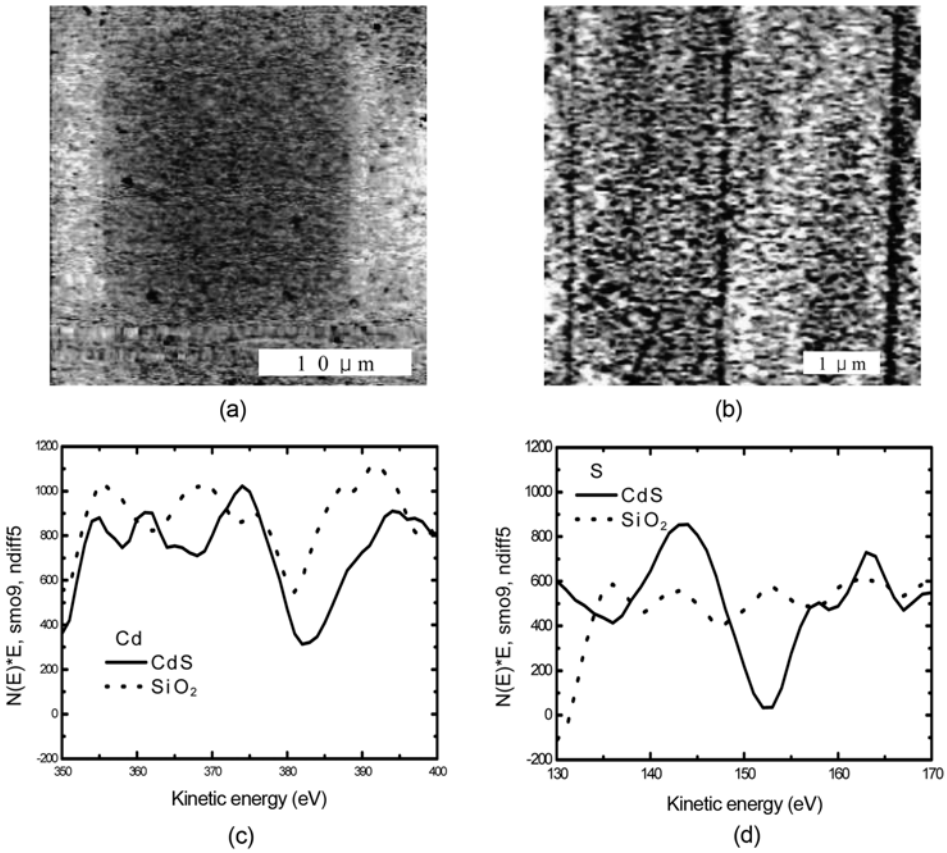

Fig. 11. LFM images of CdS square and lines via DPN method and AES multiple spectra of SiO_2 surface and CdS on silicon dioxide: (A) 20×20 μm^2 CdS area on SiO_2 substrate (1 Hz for 2 h), (b) 50, 80, and 100 nm CdS lines (left to right, 5 μm long) formed after exposure to H_2S for 1 h, (c) AES spectra of cadmium in (a), and (d) AES spectra of sulfur in (a).

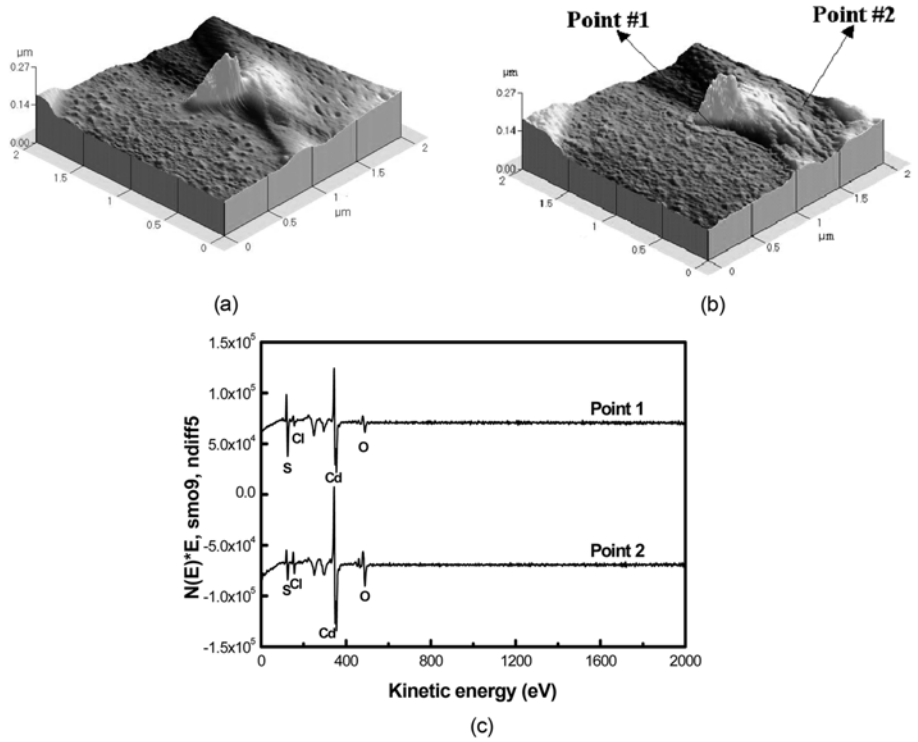

Fig. 12. AFM images of $CdCl_2$ on Au (a) and CdS crystal growth on its surface after exposure to H_2S for 2 h (b). Auger electron spectra of CdS surface at different points (c).

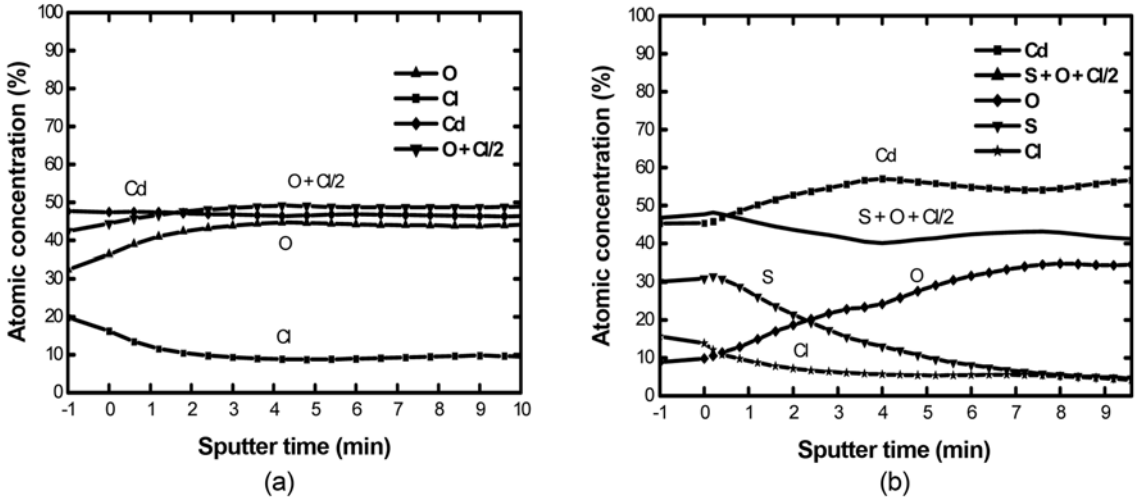

Fig. 13. AES depth profiles of precipitated $CdCl_2$ (a) and after H_2S exposure of (a) for 3 min (b) with sputter rate of 25 Å/min in SiO_2.

Above profiles show that the surface of precipitate is made of $CdCl_2$ as well as $CdCl_2 \cdot 4Cd(OH)_2$ as the water is evaporated in $CdCl_2$ solution [29]. The AES depth profile which is shown in Fig. 13(b) after exposure H_2S gas to the sample of Fig. 13(a) depicts that the reaction is mostly localized to occur in the surface. The sulfur concentration is lower and oxygen concentration is higher in the inner side of the surface when compared to those on the surface. Hence, it can be concluded that the patterns formed via DPN are in the form of CdS crystals of which thickness is in the range of 5-10 Å.

CONCLUSIONS

We fabricated CdS thin films at room temperature and atmospheric pressure using the methods assisted by Langmuir deposition, self-assembly, and DPN techniques. LB films of saturated arachidic acid and LS films of unsaturated PCDA were reacted with cadmium ions and exposed to H_2S gas. After the reaction with H_2S gas, the crystallization of CdS on solid substrates was confirmed by the complete disappearance of the carboxylate band and the recovery of the carbonyl band. Also, the increase of surface roughness from 2.6 Å to 7.3 Å strongly suggests that CdS growth occurs by an exposure to H_2S gas. When the SAMs were utilized for the deposition of CdS colloidal particles, MHA was self-assembled on Au substrate to act as a receptor layer. At pH=9.1, the density of immobilized CdS particles was relatively higher compared to that obtained at pH= 5.0. Nanometer-scale crystals of CdS were successfully deposited with predetermined pattern at target local positions by using $CdCl_2$-coated AFM tips. This technique has an advantage in exquisite control of fabricating smaller semiconductor crystal patterns.

ACKNOWLEDGMENT

This work was supported by the Korea Research Foundation (Center for Integrated Nano Systems (KRF-R0406243)), Ministry of Science & Technology (Protein Chip Technology program (MOST-R0608431) and Center for Ultramicrochemical Process System (R11-2001-089-07001)), Ministry of Health and Welfare (MOHA050750), and the Korea Foundation for International Cooperation of Science and Technology (KICOS-K2071700007707B010007710).

NOMENCLATURE

AES : auger electron microscopy
AFM : atomic force microscope
DPN : Dip-pen nanolithography
FTIR : fourier transform infrared
LB : Langmuir-Blodgett
LS : Langmuir-Schaefer
MHA : mercaptohexadecanoic acid
MMA : mean molecular area
PCDA : 10,12-pentacosadiynoic acid
SAMs : self-assembled monolayers
SEM : scanning electron microscope
SPL : scanning probe lithography

REFERENCES

1. Z. L. Wang, *Characterization of nanophase materials*, WILEY-VCH, Weinheim, 1st ed., 315 (2000).
2. Z. Han, Q. Yang, J. Shi, G. Q. Lu and S. W. Lewis, *Solid State Sci.*, **10**, 563 (2008).
3. J. Frenzel, J.-O. Joswig and G. Seifert, *J. Phys. Chem. C*, **111**, 10761 (2007).
4. G. Li, L. Jiang, H. Peng and B. Zhang, *Mater. Lett.*, **62**, 1881 (2008).
5. Y. Wang and N. Herron, *J. Phys. Chem.*, **95**, 525 (1991).
6. X. Xu, J. Cesarano III, E. Burch and G. P. Lopez, *Thin Solid Films*, **305**, 95 (1997).
7. K. S. Ramaiah, V. S. Raja and M. Sharon, *J. Mater. Sci.: Mater. El.*, **9**, 261 (1998).
8. R. W. Corkery, *Langmuir*, **13**, 3591 (1997).
9. T. Richardson, C. McCartney, N. Cowlam, F. Davis, D. J. M. Stirling, A. K. Ray, V. Gacem, A. Gibaud and A. V. Nabok, *Thin Solid Films*, **327-329**, 510 (1998).
10. G. Roberts, *Langmuir-blodgett films*, Plenum Press, New York, NY (1990).
11. D. J. Ahn, E.-H. Chae, G. S. Lee, H.-Y. Shim, T.-E. Chang, K.-D.

Ahn and J.-M. Kim, *J. Am. Chem. Soc.*, **125**, 8976 (2003).
12. J. Sagiv, *J. Am. Chem. Soc.*, **102**, 92 (1980).
13. C. P. Tripp and M. L. Hair, *Langmuir*, **11**, 1215 (1995).
14. Y. Xia and G. M. Whitesides, *Angew. Chem. Int. Edit.*, **37**, 550 (1998).
15. A. Bernard, J. P. Renault, B. Michel, H. R. Bosshard and E. Delamarche, *Adv. Mater.*, **12**, 1067 (2000).
16. L. Guo, P. R. Krauss and S. Y. Chou, *Appl. Phys. Lett.*, **71**, 1881 (1997).
17. M. Li, L. Chen and S. Y. Chou, *Appl. Phys. Lett*, **78**, 3322 (2001).
18. S. Kramer, R. R. Fuierer and C. B. Gorman, *Chem. Rev.*, **103**, 4367 (2003).
19. P. A. Brooksby and A. J. Downard, *Langmuir*, **21**, 1672 (2005).
20. A. Bezryadin and C. Dekker, *J. Vac. Sci. Technol. B*, **15**(4)**,** 793 (1997).
21. R. D. Piner, J. Zhu, F. Xu, S. Hong and C. A. Mirkin, *Science*, **283**, 661 (1999).
22. K. S. Salaita, S. W. Lee, D. S. Ginger and C. A. Mirkin, *Nanolett.*, **6**, 2493 (2006).
23. D. S. Ginger, H. Zhan and C. A. Mirkin, *Angew. Chem. Int. Edit.*, **43**, 30 (2004).
24. S. K. Kwak, G. S. Lee, D. J. Ahn and J. W. Choi, *Mat. Sci. Eng. C*, **24**, 151 (2003).
25. V. Vogel and W. Christof, *J. Chem. Phys.*, **84**, 5200 (1986).
26. J. Y. Hyun, G. S. Lee, T. Y. Kim and D. J. Ahn, *Korean J. Chem. Eng.*, **14**, 533 (1997).
27. V. Erokhin, P. Facci, S. Carrara and C. Nicolini, *J. Phys. D: Appl. Phys.*, **28**, 1 (1997).
28. S. Boussaad, L. Dziri, R. Arechabaleta, N. J. Tao and R. M. Leblanc, *Langmuir*, **14**, 6215 (1998).
29. N. N. Greenwood and A. Earnshaw, *Chemistry of the elements*, Pergamon Press, 1st ed., 1395 (1984).